Microwave Magnetic-Transmission Resonance in Gadolinium†

George C. Alexandrakis* and Thomas R. Carver
Palmer Physical Laboratory, Princeton University, Princeton, New Jersey 08540

and

Owen Horan‡
Department of Physics, University of Miami, Coral Gables, Florida 33124
(Received 11 September 1969; revised manuscript received 23 August 1971)

Transmission-resonance experiments are described in paramagnetic and ferromagnetic gadolinium with a Curie point $T_C \cong 289$ °K. In these experiments, utilizing the spin-transmission-resonance technique, transmission resonance occurs not by diffusion of spins, but by modulation of the microwave penetration depth under resonance conditions. The effect is related to "antiresonance" previously observed in some cases of ferromagnetic resonance, but is much more pronounced in the transmission technique. A simple theory, due to VanderVen, and the solution of the boundary-value problem, due to Alexandrakis, accurately describe the results for paramagnetic gadolinium, and the fitted data yield several experimental parameters, in particular the relaxation time, as well as the susceptibility and resistivity. However, preliminary results indicate that these theories are inadequate to describe the transmission signals in ferromagnetic cases, even though they are adequate to fit the conventional absorption-resonance signals.

I. INTRODUCTION

The spin-transmission-resonance technique was originally introduced to aid in the observation of conduction-electron spin resonance (CESR) in metals.[1,2] The technique helps to overcome skin-depth and sample-impurity problems, and is considerably more sensitive than conventional absorption resonance in certain cases. This technique, which has been described previously,[3] in experimental detail and in theory in a number of articles,[3–6] is described, roughly, as follows. Resonance signals are carried from a microwave-excitation cavity by diffusing precessing spins through a sample, which is much thicker than the normal skin depth, to a receiving cavity connected to a phase-sensitive homodyne receiver. The line shape then depends on a fixed diffusion thickness.

However, it is not necessary that the precessing spins actually be able to diffuse. In this paper we describe transmission phenomena in paramagnetic and ferromagnetic resonance in which large and interesting signals are transmitted by the modulation (particularly the increase) of the normal skin depth by the magnetic susceptibility of the material. This effect, which we might call magnetic-dispersion skin-depth modulation (MDSDM) and which is related to "antiresonance" in ferromagnetic resonance,[7] was discovered in gadolinium in an experimental search for spin-wave transmission,[8] and was originally misinterpreted. Subsequent measurements of the skin depth and assistance from other sources[9–11] led to the correct explanation. A theory for paramagnetic materials correctly and accurately accounts for line shapes in gadolinium. If we try to adapt this theory to fit ferromagnetic materials by taking the z component of the magnetization to be M_s, the saturation magnetization, rather than χH_z, it does not agree with experiment at all. This is discussed in Sec. V B, where the ferromagnetic-resonance situation is reviewed.

Before describing the theory and details of the experimental results, it is useful to describe the phenomenon in simple terms. Consider a sample of paramagnetic material such as gadolinium, which contains paramagnetic ion cores and conduction electrons. These electrons are assumed to give the sample a microwave skin depth smaller than its thickness and yet have negligible paramagnetic susceptibility of their own. Gadolinium has an atomic number $Z = 64$ and its electron configuration contains the terms $4f^7 5d^1 6s^2$ outside the xenon-atom configuration $(1s^2 2s^2 2p^6 3s^2 3p^6 3d^{10} 4s^2 4p^6 4d^{10} 5s^2 5p^6)$. The ground state of Gd^{3+} is $^8S_{7/2}$. According to all facts known for Gd and the other magnetic rare earths, the electrons responsible for the strong paramagnetism[12,13] above the Curie temperature, as well as for the ferromagnetism[14] below this temperature, are the $4f$ electrons which almost entirely retain their localized atomic character. The Gd ferromagnetism is sustained through the indirect-exchange interaction between the collective $5d^1$ and $6s^2$ electrons and the localized $4f^7$ electrons. Calculations have shown[15] that the free-electron spin-relaxation time in ferromagnets is too short to permit any diffusion of polarized spins through a thickness comparable to the sample's thickness. The dynamic skin depth in the material is given by $\delta = c/(2\pi\sigma\omega\mu)^{1/2}$. The permeability $\mu = 1 + 4\pi(\chi' - i\chi'')$, where χ', χ'' are the real and imaginary parts

of the dynamic susceptibility, depends on a frequency-dependent $\chi'(\omega-\omega_0)$, and when $1+4\pi\chi'\times(\omega-\omega_0)<1$, the skin depth is increased. From the causal properties of $\chi'(\omega-\omega_0)$, this happens on the high-frequency side of ω_0, where ω_0 is the resonant frequency, and, if the frequency is fixed and the magnetic field varied, on the low-field side of $H_0=\omega_{rf}/\gamma$. In gadolinium, the skin depth at room temperature is about 4 μ. A typical sample might be 15 skin depths, or 60 μ thick. A typical excitation cavity power of 100 mW incident on one side of the sample will give a skin-depth leakage into the receiver cavity of about 10^{-13} W, and any variation of the skin depth will produce a noticeable signal. Moreover, because of exponential e folding, a small fractional change in the skin depth will result in a fractional change in transmitted signal which is greater by the ratio of the thickness to the skin depth—a factor of 15 in the above example.

Another interesting feature of MDSDM is the changed nature of demagnetization effects. The torque on a magnetization vector $\vec{M}$ is given by $\dot{\vec{M}}=\gamma(\vec{M}\times\vec{B})$, but because the magnetization, in the case of absorption, is assumed to comprise part of the field $\vec{B}$ and because $\vec{M}\times\vec{M}=0$, the precession equation[16] is $\dot{\vec{M}}=\gamma(\vec{M}\times\vec{H})$, where $\vec{H}$ is the field inside the material. From this equation, it is well known that resonance absorption occurs for a field $H_0=H_a-4\pi M$ when H_a, the static externally applied magnetic field, is normal to the sample surface, and occurs for a field $H_0=[H_a(H_a+4\pi M)]^{1/2}$ when H_a is parallel to the sample surface. Here $H_0=\omega/\gamma$ is the field at which resonance would take place in the absence of demagnetization effects. These effects are, of course, surface effects arising from the electromagnetic boundary conditions and, in the case of the *transmitted* signal, they are not present because the transmitted MDSDM signal is not a surface effect. It is a bulk resonance effect which is indirectly coupled to the applied microwave field through the eddy currents. As a consequence, the transmitted signal resonance occurs for a magnetic field related to the $\vec{B}$ field inside the sample. When the static magnetic field is parallel to the sample surface, H inside the sample is equal to H_a and transmission resonance occurs when $B_{ins}=H_0$, corresponding to an applied field much less than H_0. When, however, the static field is normal to the sample, B_{ins} is equal to the applied field H_a, so the transmission resonance occurs when $H_a=H_0$. The situation is shown schematically in Fig. 1.

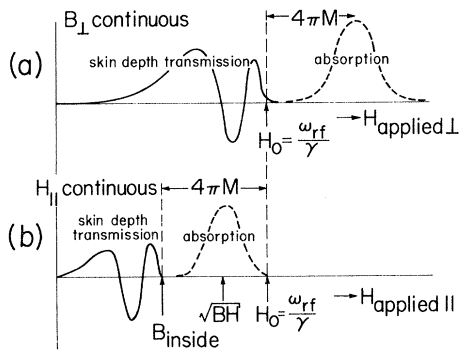

FIG. 1. Schematic representation of transmission and absorption resonance shifts: (a) perpendicular field case, (b) parallel field case.

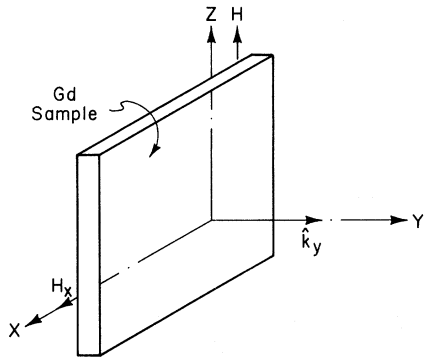

FIG. 2. Parallel field geometry.

II. THEORY

A. Determination of Propagation Constants

Since we are interested in describing the propagation of microwaves inside a magnetic material, we must take into account some equation besides the eddy-current equation to describe the magnetic resonance of the electron spins under the influence of the microwaves. Following VanderVen[11] we shall use the Bloch-Bloembergen equation to describe the magnetic resonance. We have

$$\nabla\times(\nabla\times\vec{H})=\frac{-4\pi\sigma}{c^2}\frac{\partial}{\partial t}(\vec{H}+4\pi\vec{M}), \tag{1}$$

$$\frac{\partial\vec{M}_t}{\partial t}=\gamma(\vec{M}\times\vec{H})_t-\frac{\vec{M}_t}{\tau}, \tag{2}$$

where the subscript t in Eq. (2) indicates components transverse to the direction of the static applied magnetic field and τ is therefore the transverse relaxation time. In writing Eq. (1) we have assumed that $\vec{J}=\sigma\vec{E}$ and the contribution of the displacement current is negligible, i.e., $\sigma\gg\epsilon\omega$.

The calculations are done for paramagnetic metals so $M_z=\chi H_a$. We assume $H_{x,y}$ and $M_{x,y}$ $\sim e^{i(\vec{k}\cdot\vec{r}+\omega t)}$ and that the magnitude of the microwave parts of the magnetic field and magnetization are much smaller than the static components, i.e., $|H_{x,y}|\ll H_z$ and $|M_{x,y}|\ll M_z$.

We start with the static magnetic field parallel

to the sample surface.

1. *Parallel Field Case*

Consider that the Gd sample lies in the xz plane and that the static applied field H_a is along the z axis. Furthermore, take the magnetic component of the linearly polarized microwaves inside the excitation cavity to be along the x axis as shown in Fig. 2.

From the boundary conditions on $\vec{B}$ and $\vec{H}$ and the fact that there is no external magnetic field in the y direction, we have for the field inside the sample

$$\vec{H}_{\text{ins}} = H_x\hat{i} - 4\pi M_y\hat{j} + H_a\hat{k}.$$

Therefore, Eqs. (1) and (2) in component form give us the set of equations

$$(k^2 + 2i/\delta^2)H_x + (8\pi i/\delta^2)M_x = 0, \tag{3a}$$

$$(i\omega\tau + 1)M_x - \gamma\tau H_a(1 + 4\pi\chi)M_y = 0, \tag{3b}$$

$$\gamma\tau H_a M_x - \gamma\tau\chi H_a H_x + (i\omega\tau + 1)M_y = 0, \tag{3c}$$

where δ is the classical skin depth given by $\delta^2 = c^2/2\pi\sigma\omega$.

For Eqs. (3) to have solutions for H_x, M_x, and M_y, the determinant of the coefficients must vanish. This gives us the following expression for k^2:

$$k^2 = \frac{-2i}{\delta^2}\left(\frac{1 + 2i\gamma\tau H_0 + [H_a^2(1 + 4\pi\chi)^2 - H_0^2]\gamma^2\tau^2}{1 + 2i\gamma\tau H_0 + [H_a^2(1 + 4\pi\chi) - H_0^2]\gamma^2\tau^2}\right), \tag{4}$$

where we have used $\omega = \gamma H_0$. It is clear from the above equation that k^2 will be a maximum for

$$H_0 = H_a(1 + 4\pi\chi)^{1/2} \quad \text{or} \quad \omega = \gamma(BH)^{1/2}. \tag{5}$$

Since the real part of the surface impedance is proportional to the imaginary part of k, when k is large the microwave absorption will be large. That is, at $\omega = \gamma(BH)^{1/2}$ we shall have absorption resonance in exact analogy with ferromagnetic absorption resonance.[16] On the other hand, when $H_0 = H_a(1 + 4\pi\chi)$, k will be small and the transmission of the microwaves through the sample will be high. In other words, transmission resonance will occur at $B = H_0$.

2. *Perpendicular Field Case*

Let us now take the Gd sample to lie in the xy plane, the static magnetic field to lie along the z axis, and the microwave field to oscillate along the x axis as shown in Fig. 3. Again taking into account the boundary conditions for the fields $\vec{B}$ and $\vec{H}$ we obtain

$$\begin{aligned} &B_z(\text{out}) = B_z(\text{in}), \\ &H_a = H_z + 4\pi M_z. \end{aligned} \tag{6}$$

Assuming $M_z = \chi H_a$, we have

$$H_z = H_a(1 - 4\pi\chi). \tag{7}$$

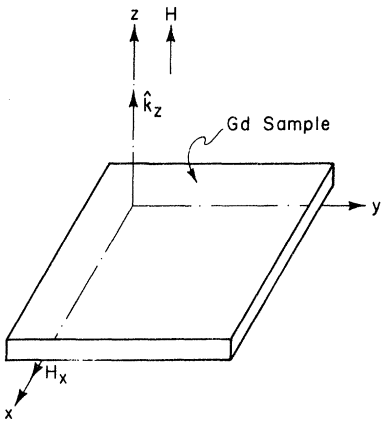

FIG. 3. Perpendicular field geometry.

The field inside the sample is

$$\vec{H}_{\text{ins}} = H_x\hat{i} + H_y\hat{j} + H_a(1 - 4\pi\chi)\hat{k}. \tag{8}$$

Equations (1) and (2) for this case give us the set of four equations:

$$\begin{aligned} &(k^2 + 2i/\delta^2)H_x + (8\pi i/\delta^2)M_x = 0, \\ &(k^2 + 2i/\delta^2)H_y + (8\pi i/\delta^2)M_y = 0, \\ &(i\omega\tau + 1)M_x - \gamma\tau H_a[(1 - 4\pi\chi)M_y - \chi H_y] = 0, \\ &(i\omega\tau + 1)M_y - \gamma\tau H_a[\chi H_x - (1 - 4\pi\chi)M_x] = 0. \end{aligned} \tag{9}$$

Defining

$$H_n = \tfrac{1}{2}(H_x - iH_y), \quad H_p = \tfrac{1}{2}(H_x + iH_y)$$

and

$$M_n = \tfrac{1}{2}(M_x - iM_y), \quad M_p = \tfrac{1}{2}(M_x + iM_y),$$

Eqs. (9) decouple into the two sets

$$\begin{aligned} &(k^2 + 2i/\delta^2)H_n + (8\pi i/\delta^2)M_n = 0, \\ &(i\omega\tau + 1)M_n - i\gamma\tau H_a[(1 - 4\pi\chi)M_n - \chi H_n] = 0 \end{aligned} \tag{10}$$

and

$$\begin{aligned} &(k^2 + 2i/\delta^2)H_p + (8\pi i/\delta^2)M_p = 0, \\ &(i\omega\tau + 1) + i\gamma\tau H_a[(1 - 4\pi\chi)M_p - \chi H_p] = 0. \end{aligned} \tag{11}$$

The determinant of the coefficients of H_n and M_n in Eq. (10) and of H_p and M_p in Eq. (11) must be zero for solutions to exist. Thus we have the two solutions for k^2:

$$k_n^2 = \frac{-2i}{\delta^2}\left(\frac{1 + i\gamma\tau(H_0 - H_a)}{1 + i\gamma\tau[H_0 - H_a(1 - 4\pi\chi)]}\right), \tag{12}$$

$$k_p^2 = \frac{-2i}{\delta^2}\left(\frac{1 + i\gamma\tau(H_0 + H_a)}{1 + i\gamma\tau[H_0 + H_a(1 - 4\pi\chi)]}\right). \tag{13}$$

Looking at Eqs. (12) and (13) we see immediately that (12) will exhibit resonance behavior while (13) cannot. k_n will have an absorption resonance given

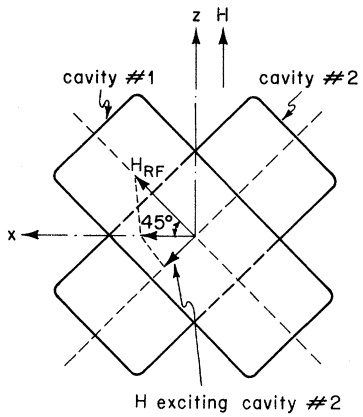

FIG. 4. Geometry of cavities and fields in the parallel field case.

by $H_a = H_0/(1 - 4\pi\chi)$ and a transmission resonance at $H_a = H_0 = B$.

B. Solution of Boundary Conditions

We wish to determine the amplitude of the microwave magnetic field transmitted through the sample and detected by the receiver. To do this we use the fact that the tangential components of $\vec{E}$ and $\vec{H}$ must be continuous across any boundary. Using

$$\vec{\nabla}\times\vec{H} = \frac{4\pi}{c}\vec{J} + \frac{1}{c}\frac{\partial\vec{D}}{\partial t}$$

and our previous assumptions we can express $\vec{E}$ in terms of $\vec{H}$:

$$\vec{E} = a(\vec{k}\times\vec{H}), \tag{14}$$

where

$$a = ic/(4\pi\sigma + i\epsilon\omega)\ . \tag{15}$$

Note that for air $\sigma \approx 0$ and $\epsilon \approx 1$ so Eq. (15) becomes for air

$$a_0 = c/\omega\ , \tag{16}$$

and for most metals, since $\sigma \gg \epsilon\omega$, we have

$$a_m = ic/4\pi\sigma. \tag{17}$$

Now we are ready to treat the two geometries.

1. *Parallel Field Case*

The experimental situation for this case is represented in Fig. 4. The static applied magnetic field H_a is parallel to the surface of a Gd foil which lies in the xz plane such that the incident microwave field of the exciting cavity makes a 45° angle as shown. Consequently, the x component of the incident microwave field is

$$H_{ix} = \tfrac{1}{2}\sqrt{2}\,H_{rf}\ . \tag{18}$$

The z component is obviously equal to the x component.

To find the field which excites the receiving cavity (cavity No. 2 in Fig. 4) we must take the projection of the x and z components of the transmitted fields H_{tx} and H_{tz} on the long axis of cavity No. 2. Again the angle is 45°, which means the total transmitted field is

$$H_t = \tfrac{1}{2}\sqrt{2}\,(H_{tx} - H_{tz}). \tag{19}$$

Now we can determine H_{tx} and H_{tz} using the boundary conditions on $\vec{E}$ and $\vec{H}$. Using Eq. (14) we express E_z in terms of H_x and obtain the system of equations

$$\begin{aligned}
&H_{ix} + H_{rx} = H_x^+ + H_x^-,\\
&a_0k_0(H_{ix} - H_{rx}) = a_m k(H_x^+ - H_x^-),\\
&H_{tx}e^{ik_0d} = H_x^+ e^{ikd} + H_x^- e^{-ikd}\ ,\\
&a_0k_0H_{tx}\,e^{ik_0d} = a_m k(H_x^+ e^{ikd} - H_x^- e^{-ikd})\ ,
\end{aligned} \tag{20}$$

for the boundary conditions. H_{ix} and H_{rx} are the x components of the amplitudes of the incident and reflected waves; H_x^+ and H_x^- are the x components of the amplitudes of the waves traveling to the right and left, respectively, in the metal; k_0 is the propagation constant of the waveguide; and d is the thickness of the metal foil. Solving the set of Eqs. (20) for H_{tx} we get

$$H_{tx} = 2a_0k_0H_{ix}\,\frac{a_m k e^{-ik_0d}}{2a_0k_0a_m k\cos kd - (a_0^2k_0^2 + a_m^2k^2)i\sin kd}\ . \tag{21}$$

The solution for H_{tz} is the same, but with k replaced by k'. k' is the usual propagation constant for a metal:

$$k' = (1 - i)/\delta\ .$$

The z component H_{tz} is therefore just the leakage through the metal foil. Using Eqs. (16)–(19) and the definition of δ, the total transmitted field is given by

$$H_t = \tfrac{1}{2}H_{rf}k_0e^{-ik_0d}\left(\frac{k}{f_x} - \frac{k'}{f_z}\right), \tag{22}$$

where

$$f_x = k_0k\cos kd - \left[\left(\frac{k_0c}{\delta\omega}\right)^2 - \left(\frac{\delta\omega k}{2c}\right)^2\right]i\sin kd,$$

with a similar expression for f_z with k again replaced by k'.

The experimental apparatus amplifies the signal by a factor A and introduces a phase shift ϕ. Therefore, the measured field amplitude will be given by

$$H_t = \mathrm{Re}\left[\frac{A}{2}\,H_{rf}\,k_0e^{-i(k_0d+\phi)}\left(\frac{k}{f_x} - \frac{k'}{f_z}\right)\right]. \tag{23}$$

2. *Perpendicular Field Case*

The geometry of the experimental situation for

this case is shown in Fig. 3. It is obvious that $H_{ix} = H_{rf}$ and $H_{iy} = 0$. This means, from the definitions for H_n and H_p, that $H_{ip} = H_{in} = \frac{1}{2} H_{rf}$.

The equations for the boundary conditions on H_n and H_p are essentially the same as those for H_x and H_z in the parallel field case. So we have solutions similar to Eq. (21) for each H_n and H_p. The receiving cavity supports oscillations only along the y axis (crossed cavities) so, again from the definition of H_n and H_p we have

$$H_{ty} = i(H_n - H_p). \tag{24}$$

Again we have amplification and phase shifting by the apparatus so the measured field amplitude is

$$H_{ty} = \mathrm{Re}\left[iAH_{rf} k_0 e^{-i(k_0 d + \phi)}\left(\frac{k_n}{f_n} - \frac{k_p}{f_p}\right)\right]. \tag{25}$$

An alternative quantum-mechanical calculation has been done[17] using a Green's-function approach assuming only the uniform precession mode (magnon wave number $k \approx 0$) to be important. Instead of using the equation of motion [Eq. (2)] for the magnetization, the susceptibility tensor is derived. The results of this magnon theory are identical to the ones obtained here.

III. EXPERIMENTS IN GADOLINIUM

A. Apparatus and Samples

The heart of the transmission-resonance apparatus is the double-cavity structure with the sample making a common wall between the two cavities. One cavity acts as an excitation cavity, and the second cavity acts as an impedance match between the metallic sample and the receiver. The cavities and phase-sensitive receiver have been fully described in a previous paper (Ref. 3) and will not be described here. However, the particular cavity which was used in these experiments is illustrated in Fig. 7 of Ref. 3. In this structure the directions of the microwave magnetic fields in each cavity are mutually perpendicular, although in the plane of the sample. Thus leakage is reduced. When the static field is in the sample plane (the parallel field case) a component of the exciting field which is perpendicular to the static field is transmitted to the other under resonance conditions. When the static field is in the perpendicular direction, transmission depends on the helicity of the fields propagating through the sample. That this occurs for CESR is obvious from the precession of spins. It also occurs and has been taken into account in the detailed calculations for the case of MDSDM.

Gadolinium foil is placed between two brass plates with circular holes, approximately 1 cm in diameter, milled in them. Each plate contains two O-ring grooves made to fit indium wire rings. The outer ring seals the brass plate to the cavity block, and the inner ring, made just slightly larger than the hole, seals the brass plate to the foil. When the plates and sample foil are clamped tightly together the cavities become microwave leak tight and even liquid-helium tight.

Gadolinium foils of 99.9% purity were obtained from the Research Chemical Co.[18] A number of different foil thicknesses were tried, but no significant variations appeared in the fitted parameters. Consequently, the data presented here is from 60-μ-thickness foils which provided interesting and detailed line shapes characterized by a large thickness-to-skin-depth ratio, and yet were thin enough to give an excellent signal-to-noise ratio. Samples as thick as 75 μ produced weak signals, and samples as thin as 25 μ produced large leakage powers which degraded the receiver by saturation.

B. Experimental Results

The experimental results for the two orientations of the external dc magnetic field are shown in Figs. 5 and 6. On the figures, the transmission signals are denoted by TRA and the absorption or reflection signals by REF.

1. *Parallel Field Case*

The first striking feature of the data in Fig. 5 is that for any temperature the absorption and transmission resonances appear at different values for the external dc magnetic field. We further observe that even for temperatures above the Curie point, $T_C = 289\,^{\circ}\mathrm{K}$, the absorption resonance appears below the dc field value which, for our microwave frequency $\nu = 9.2$ GHz, corresponds to a g factor of 2. The resonance field value H_0 for this frequency and $g = 2$ is 3280 G (see Introduction).

Other features of the experimental results for this case are that the absorption resonance moves closer to the H_0 field value when the temperature increases and moves away from it as the temperature decreases. Also, the profile of the transmission resonance changes substantially as a function of temperature.

Comparing the transmission resonance with the absorption resonance we see that the former has a larger signal-to-noise ratio as well as a more complex structure. These two features are indispensable in obtaining a reliable analysis of experimental data.

Finally, we observe that the transmission resonance in the parallel field case is not attenuated very drastically below the Curie point, contrary to previous suggestions.[10] Furthermore, the transmission resonance does not begin to appear immediately above $H_a = 0$ in the low-temperature region.

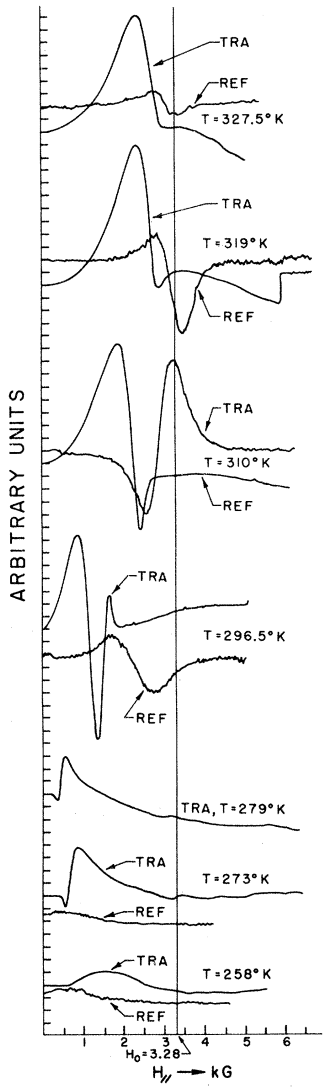

FIG. 5. Experimental resonances in Gd for parallel applied field. Transmission (TRA) and reflection (REF) resonances at various temperatures.

The signal strength with the sample at room temperature was approximately 120 dB below the klystron power level.

2. *Perpendicular Field Case*

In Fig. 6 we observe that the transmission resonance starts to appear immediately as H_a increases from zero, while the absorption resonance does not begin to appear until H_a approaches H_0 or exceeds it.[19] The absorption resonance decreases its linewidth and moves closer to H_0 as the temperature increases and, as is indicated above, suffers strong attenuation below the Curie point. The resonance transmission profile changes drastically with temperature. Finally, it is worth noticing that although the width of the absorption resonance increases substantially as the temperature decreases, the width of the transmission resonance remains essentially constant. The signal strength for $T > T_C$ was about the same as in the parallel field case.

IV. COMPARISON OF EXPERIMENTAL LINE SHAPE WITH THEORY

We are now ready to compare the experimental results with the theory developed in Sec. II.

1. *Parallel Field Case*

Equation (23) is the theoretical signal expression for this case. A digital computer, programmed with a nonlinear least-squares-fitting routine,[20] was used to fit the theory to the experimental data.

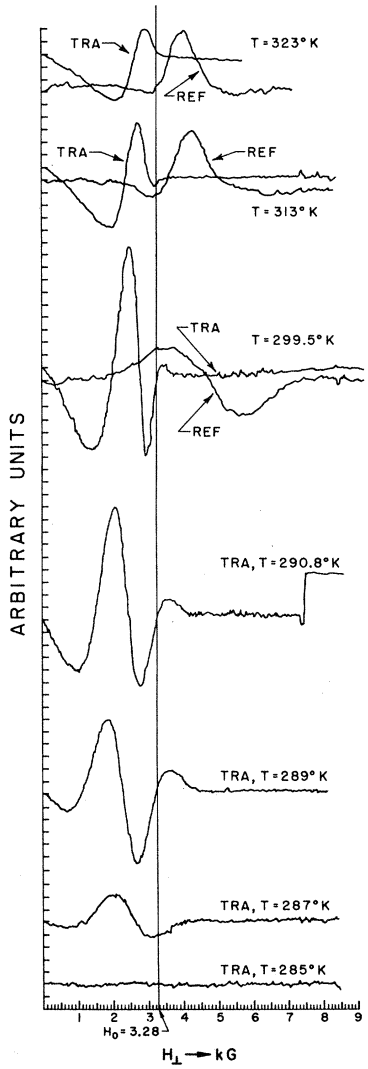

FIG. 6. Experimental resonances in Gd for perpendicular applied field. Transmission and reflection resonances at various temperatures.

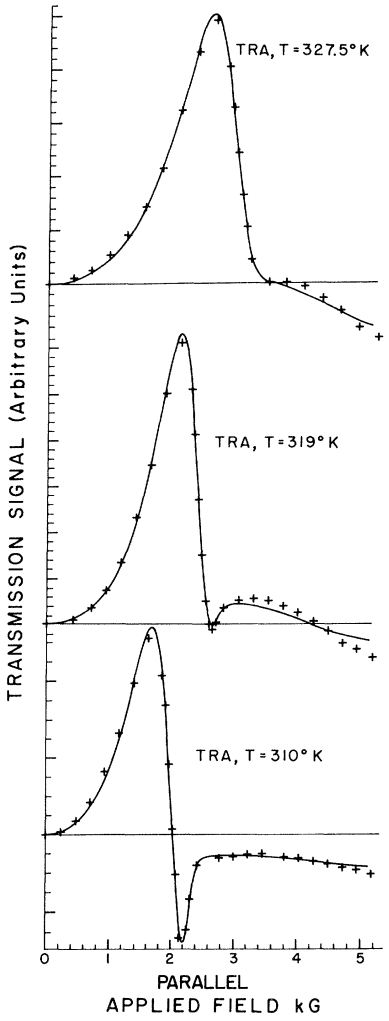

FIG. 7. Computer-fitted Gd data for parallel applied field at various temperatures. Crosses are experimental points from the traces of Fig. 5. The continuous line is computed from Eq. (22). The best fit parameters are listed in Table I.

What this routine does, essentially, is to attempt to minimize the sum of the squares of the differences between the theoretical and experimental values at each data point by looking for a minimum of the hypersurface in the space of the parameters. It starts with a set of guesses for the parameters and increments each one until a convergence criterion is satisfied or a given number of iterations has been performed.

The results for the three temperatures $T = 327.5$, 319, and 310 °K are shown in Fig. 7. The crosses are the experimental points picked from the recorded data of Fig. 5 and the continuous line is the theoretical signal calculated with the parameters obtained from the fitting program. The values of δ, χ, τ, obtained for these temperatures are given in Table I.

2. *Perpendicular Field Case*

Using Eq. (25) for the theoretical signal expression a procedure similar to the one used for the parallel case above was used to obtain the curves shown in Fig. 8 for the temperature 323, 313, and 299.5 °K.

Again, the crosses are the experimental points and the continuous line is the theoretical signal. The values of the parameters which gave the best fit are given in Table I. As can be seen from Fig. 8, the fit between theory and experiment for $T = 299.5$ °K is not as good as it is for the other temperatures. This is to be expected because the assumption that $\vec{M} = \chi\vec{H}$ with χ a constant, becomes increasingly untenable as the Curie temperature ($T_C \approx 289$ °K for Gd) is approached. For this reason, the parameters obtained from the fitting procedure for this and lower temperatures are rather dubious and have been omitted from Table I.

V. CONCLUSIONS

A. Paramagnetic Experiments

Table I contains the values of the parameter χ, τ, δ, and ρ ($\rho = 2\pi\delta^2\omega/c^2$) obtained for five different temperatures in the paramagnetic temperature region. They are plotted against temperature in Figs. 9–11. The susceptibility line in Fig. 9 seems to agree fairly well with the one obtained by Trombe.[12]

The ferromagnetic state of Gd is due to indirect exchange interactions between the s and $d(f)$ elec-

TABLE I. Fitted values of χ, τ, δ, and ρ for a Gd sample 60 μ thick and 99.9% pure.

T (°K)	χ (10^{-2})	τ (10^{-10} sec)	δ (10^{-4} cm)	ρ (10^{-4} Ω cm)	Field geometry
310	2.75 ± 0.14	1.08 ± 0.04	4.96 ± 0.21	0.89 ± 0.08	∥
313	2.39 ± 0.22	1.02 ± 0.02	5.33 ± 0.14	1.03 ± 0.05	⊥
319	2.14 ± 0.15	1.23 ± 0.06	6.75 ± 0.69	1.65 ± 0.34	∥
323	1.41 ± 0.09	1.13 ± 0.03	6.59 ± 0.26	1.58 ± 0.12	⊥
327.5	2.09 ± 0.20	1.10 ± 0.07	8.16 ± 1.11	2.42 ± 0.66	∥

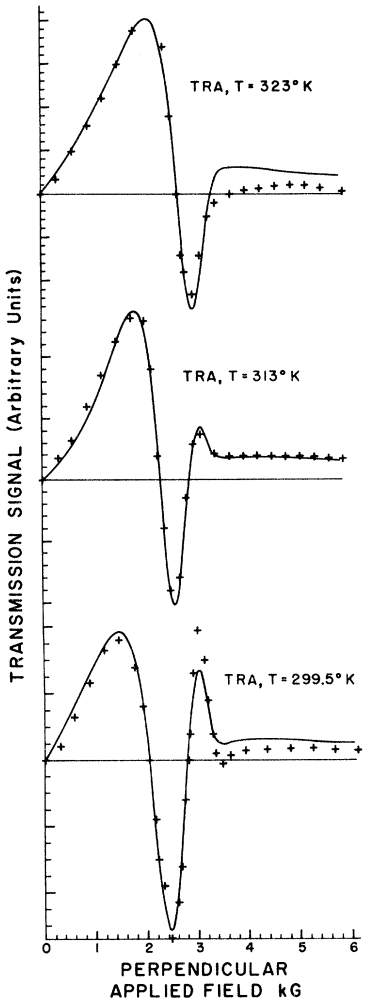

FIG. 8. Computer-fitted Gd data for perpendicular applied field at various temperatures. Crosses are experimental points from the traces of Fig. 6. The continuous line is computed from Eq. (25). The best fit parameters are listed in Table I.

trons. Thus there is a dynamic interaction between the spin waves in the ion lattice and the conduction electrons. This interaction effectively determines the relaxation processes between the two systems. The s-$d(f)$ relaxation time $\tau_{s\text{-}d(f)}$ has been found to be $\tau_{s\text{-}d(f)} \approx 10^{-10}$ sec for $\tau \approx 10\,^{\circ}\mathrm{K}$.[21] The values for τ which we have obtained for the paramagnetic temperature region would seem to indicate that relaxation even in the paramagnetic case is predominantly due to indirect s-$d(f)$ exchange. It is also possible, however, that impurities in the sample were responsible for the low values of τ that we obtained. The data for relaxation time versus temperature for Gd plotted in Fig. 10 is the first of its kind as far as the authors know.

The values for the resistivity ρ plotted in Fig. 11 are somewhat lower than the measured dc

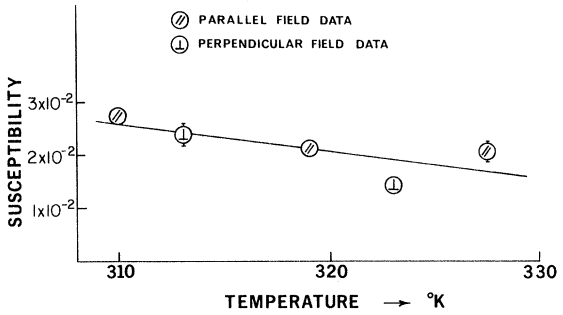

FIG. 9. Susceptibility vs temperature plotted from the fitted data in Table I.

values reported in Ref. 22. This point was also noted about lithium in Ref. 3.

A general point we would like to make about the experimental results is that the temperature was not controlled very effectively. Due to the long sweep time of the dc magnet the temperatures usually varied more than $\frac{1}{4}\,^{\circ}\mathrm{C}$ during each run. This fact could be responsible for the spread of the points in Figs. 9–11.

Summarizing the various aspects of the work performed so far we can say that the transmission resonance effect in Gd has been explained by the theory satisfactorily in the paramagnetic temperature region. It appears that transmission resonance is a useful tool for studying other ferromagnetic metals in the paramagnetic state.

B. Ferromagnetic Experiments

Besides the results on ferromagnetic transmission in Gd contained in Figs. 5 and 6, we have obtained, in collaboration with Manicopoulos, similar results[23] on ferromagnetic Fe, Ni, Co, and a high-permeability alloy with the commercial name Conetic AA. The thicknesses of these foils—about 10 μ—are somewhat smaller than those used for Gd. Phillips[24] has obtained data for Permalloy at low temperatures and Heinrich and Meshcheryakov[25]

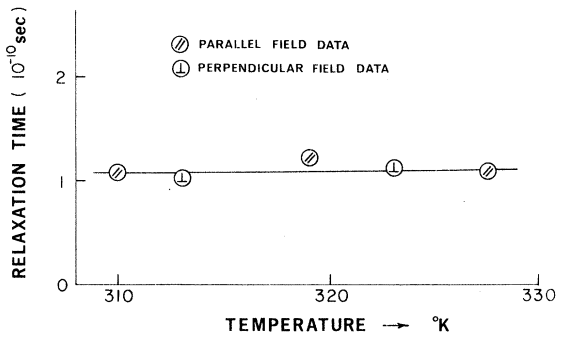

FIG. 10. Relaxation time vs temperature plotted from the fitted data in Table I.

have recently reported results from room temperature down to liquid-helium temperatures for the same alloy. The transmission line shapes obtained for these materials have many qualitative similarities to the results for the paramagnetic case.

Any theory attempting to explain ferromagnetic transmission resonance should at least contain contributions from demagnetization and exchange effects to the internal magnetic field "seen" by the spins. The approximate evolution of the ferromagnetic-resonance theory has been as follows: After the classic papers of Landau and Lifshitz, [26] Griffiths, [27] Kittel, [16] Herring and Kittel, [28] and Bloembergen, [29] we come to the work of Macdonald. [30] Macdonald was the first worker to calculate the transmission resonance for the case with the static field parallel to the sample surface and perpendicular to the microwave field, including anisotropy as well as exchange effects in his theory. He introduced the antinode boundary conditions on the magnetization and was the first one to study transmission resonance effects ferromagnetic nickel (see following discussion). His pioneering efforts had somehow escaped our attention until recently.

Ament and Rado[31] applied the Landau-Lifshitz theory, including exchange effects and antinode boundary conditions on the magnetization, and were able to obtain a value for the exchange "stiffness" constant in Permalloy by analyzing the experimental results of Rado and Weertman, [32] who used rather low values of the external field. Ament and Rado set the Landau-Lifshitz relaxation constant equal to zero to obtain the best fit to the data.

After Kittel[33] introduced the node boundary condition for the magnetization, Seavey and Tannenwald[34] observed standing spin-wave modes in thin Permalloy films and interpreted their results in terms of the Kittel boundary condition, Kaganov and Liu,[35] on the other hand, have argued that a combination of the node and antinode boundary conditions should be used in the analysis of the Rado-Weertman data because of surface quality effects.

With the discovery of ferromagnetic-transmission resonance[28] the transmission theory, including exchange and Kittel boundary conditions for the case with the static external magnetic field perpendicular to the sample surface, [24,36] has accounted qualitatively for the experimental results. We are currently continuing to work along the line of Ref. 36, hoping to establish the temperature dependence of the exchange constant and relaxation time as well as clarify the question concerning the boundary condition on the magnetization.

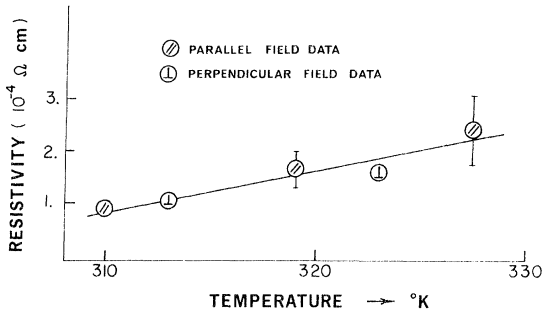

FIG. 11. Resistivity vs temperature plotted from the fitted data in Table I.

Finally, a transmission resonance effect similar to parallel pumping has been discovered[37] in ferromagnetic metals. This occurs when the static magnetic field is parallel to both the sample surface and the microwave field. It appears to be due to the excitation of certain selected spin-wave modes. [38] The fact that there is no transmission resonance when the static field is parallel to the sample surface but normal to the microwave field has been found both theoretically[39] and experimentally. [37] This can be understood from Eq. (4). By setting $M = \chi H$ we see that the numerator, which is responsible for transmission resonance, cannot "resonate" because $\gamma(H + 4\pi M) - \omega_{rf} > 0$ for the usual microwave frequencies and M values of magnetic materials.

ACKNOWLEDGMENTS

The authors are grateful to N. S. VanderVen and P. A. Fedders for their interest in the early stages of this work, and for helpful discussions at later states. We also thank C. Kittel for comments on the work and G. H. McCall for calling our attention to the general least-squares-fitting program.

†Research supported by a grant from the National Science Foundation.

*Present address: Department of Physics, University of Miami, Coral Gables, Fla. 33124.

‡NASA Predoctoral Fellow.

[1]R. B. Lewis and T. R. Carver, Phys. Rev. Letters 12, 693 (1964).

[2]N. S. VanderVen and R. T. Schumacher, Phys. Rev. Letters 12, 695 (1964).

[3]R. B. Lewis and T. R. Carver, Phys. Rev. 155, 309 (1967).

[4]M. Lampe and P. M. Platzman, Phys. Rev. 150, 340 (1966).

[5]G. D. Gaspari, Phys. Rev. 151, 215 (1966).

[6]M. B. Walker (private communication); and unpublished.

[7]W. H. Yager and F. R. Merritt, Phys. Rev. 75, 318 (1949).

[8]R. B. Lewis, G. C. Alexandrakis, and T. R. Carver, Phys. Rev. Letters 17, 854 (1966).

[9]C. Kittel (private communication).

[10]L. L. Hirst, Phys. Rev. Letters 18, 229 (1967).

[11]N. S. VanderVen, Phys. Rev. Letters 18, 277 (1967).

[12]F. Trombe, Ann. Phys. (Paris) 7, 385 (1937).

[13]S. V. Vonsovskiĭ and Yu. A. Izyumov, Usp. Fiz.

Nauk 77, 377 (1962) [Sov. Phys. Usp. 5, 547 (1963), Paper I]; 78, 3 (1962) [5, 723 (1963), Paper II].
[14]J. F. Elliott, S. Legvold, and F. H. Spedding, Phys. Rev. 91, 28 (1953).
[15]L. L. Hirst, Phys. Rev. 141, 503 (1966).
[16]C. Kittel, Phys. Rev. 73, 155 (1948).
[17]G. C. Alexandrakis, following paper, Phys. Rev. B 5, 3481 (1972).
[18]Address of Gd supplier: Research Chemicals, P.O. Box 14588, Phoenix, Ariz. 85031.
[19]A. F. Kip, C. Kittel, A. M. Portis, R. Barton, and F. H. Spedding, Phys. Rev. 89, 518 (1953).
[20]R. H. Moore and R. K. Zeigler, Los Alamos Scientific Laboratory Report No. LA-2367, 1959 (unpublished); also, Paul McWilliams, Los Alamos Scientific Laboratory Report No. LA-2367 (add.), 1962 (unpublished). The actual program used contained modifications by G. H. McCall, D. Benson, and R. K. Crawford of Princeton University, with further modifications by O. H. Horan.
[21]V. G. Bar'yakhtar and S. V. Peletminskiĭ, Zh. Eksperim. i Teor. Fiz. 39, 651 (1960) [Sov. Phys. JETP 12, 457 (1961)].
[22]S. Legvold, F. H. Spedding, F. Barson, and J. F. Elliot, Rev. Mod. Phys. 25, 129 (1953).
[23]G. C. Alexandrakis, C. N. Manicopoulos, and T. R. Carver, Bull. Am. Phys. Soc. 14, 348 (1969).
[24]T. G. Phillips, J. Appl. Phys. 41, 1109 (1970).
[25]B. Heinrich and V. F. Meshcheryakov, Zh. Eksperim. i Teor. Fiz. 59, 424 (1970) [Sov. Phys. JETP 32, 232 (1971)].
[26]L. D. Landau and E. M. Lifshitz, Phys. Zs. Soviet Union 8, 153 (1935); *Collected Papers of L. D. Landau* (Gordon and Breach, New York, 1965), Chap. 18, p. 101; L. D. Landau, *Men of Physics*, edited by D. ter Haar (Pergamon, New York, 1965), Vol. I, p. 178.
[27]J. H. E. Griffiths, Nature 158, 670 (1946).
[28]C. Herring and C. Kittel, Phys. Rev. 81, 869 (1951).
[29]N. Bloembergen, Phys. Rev. 78, 572 (1950).
[30]J. R. Macdonald, Ph.D. thesis (Oxford University, 1950) (unpublished); Proc. Phys. Soc. (London) A64, 968 (1951); Phys. Rev. 103, 280 (1956).
[31]W. S. Ament and G. T. Rado, Phys. Rev. 97, 1558 (1955).
[32]G. T. Rado and J. R. Weertman, Phys. Rev. 94, 1386 (1954); J. Phys. Chem. Solids 11, 315 (1959).
[33]C. Kittel, Phys. Rev. 110, 1295 (1958).
[34]M. H. Seavey and P. E. Tannenwald, Phys. Rev. Letters 1, 168 (1958).
[35]M. I. Kaganov and Yu Liu, Bull. Acad. Sci. USSR 25, 1388 (1961).
[36]O. H. Horan, G. C. Alexandrakis, and C. N. Manicopoulos, Phys. Rev. Letters 25, 246 (1970).
[37]G. C. Alexandrakis, O. H. Horan, T. R. Carver, and C. N. Manicopoulos, Phys. Rev. Letters 25, 1758 (1970).
[38]C. N. Manicopoulos, Bull. Am. Phys. Soc. 16, 380 (1971).
[39]O. H. Horan and G. C. Alexandrakis (unpublished).

PHYSICAL REVIEW B VOLUME 5, NUMBER 9 1 MAY 1972

Susceptibility Tensor Components for Polycrystalline Ferromagnetic Materials*

George C. Alexandrakis†
Palmer Physical Laboratory, Princeton University, Princeton, New Jersey 08540
(Received 20 April 1970)

Using the Herring-Kittel macroscopic magnon theory, the Kubo-Tomita resonance theory, and the Bogoliubov-Tyablikov equations of motion for the Green's functions of the magnon operators, explicit expressions for the components of the dynamic magnetic-susceptibility tensor are derived. As an example, the uniform precession mode (magnon wave vector $\vec{k}=0$) of a flat polycrystalline ferromagnetic plate is examined in two geometries: the static magnetic field parallel and perpendicular to the plate's surface.

I. INTRODUCTION

Herring and Kittel[1] have shown how to express the magnetization field $\vec{M}$ of a ferromagnetic material in terms of spin density operators. Kittel[2] then extended this work using the usual Holstein-Primakoff procedure[3] and obtained $\vec{M}$ in terms of macroscopic ferromagnetic magnon operators.

The behavior of a ferromagnetic material in a relatively strong dc magnetic field, which defines the z direction, with a much weaker rf magnetic field polarized in the xy plane acting as a perturbation, is analyzed using the generalized response function theory of Kubo and Tomita.[4,5] In Ref. 5, Nozières gives an exposition of the Kubo-Tomita formula which seems to be clearer than the original author's account.

Section II gives the Hamiltonian of the system and the equations of motion for the magnon operators are obtained. In Sec. III the Kubo-Tomita formula for the susceptibility is introduced and the Fourier transforms of the magnon operators are obtained using the Bogoliubov-Tyablikov[6] equations of motion for the Green's function of the magnon operators. Substituting these into the Kubo-Tomita formulas the components of the sus-